

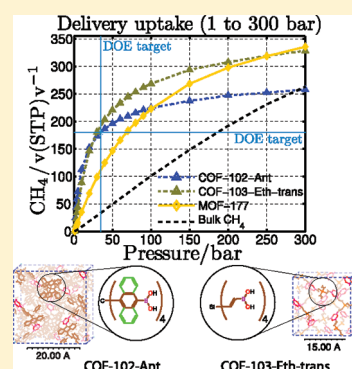
Design of Covalent Organic Frameworks for Methane Storage

Jose L. Mendoza-Cortes, Tod A. Pascal, and William A. Goddard, III*

Materials and Process Simulation Center (MC 139-74), California Institute of Technology, Pasadena, California 91125, United States

Supporting Information

ABSTRACT: We designed 14 new covalent organic frameworks (COFs), which are expected to adsorb large amounts of methane (CH_4) at 298 K and up to 300 bar. We have calculated their delivery uptake using grand canonical Monte Carlo (GCMC) simulations. We also report their thermodynamic stability based on 7.5 ns molecular dynamics simulations. Two new frameworks, COF-103-Eth-trans and COF-102-Ant, are found to exceed the DOE target of $180 v(\text{STP})/v$ at 35 bar for methane storage. Their performance is comparable to the best previously reported materials: PCN-14 and Ni-MOF-74. Our results indicate that using thin vinyl bridging groups aid performance by minimizing the interaction methane-COF at low pressure. This is a new feature that can be used to enhance loading in addition to the common practice of adding extra fused benzene rings. Most importantly, this report shows that pure nonbonding interactions, van der Waals (vdW) and electrostatic forces in light elements (C, O, B, H, and Si), can rival the enhancement in uptake obtained for microporous materials derived from early transition metals.



1. INTRODUCTION

Crystalline microporous materials systems such as the metal–organic frameworks (MOF) and covalent organic frameworks (COF) are valuable for trapping enormous amounts of gases such as H_2 , CO_2 , and CH_4 at modest pressures,^{1–7} due to their outstanding porosity. Thus COF-105 has a surface area of $6450 \text{ m}^2/\text{g}$ (equivalent to 1.4 American football fields per gram) and COF-108 has a pore volume of $5.4 \text{ cm}^3/\text{g}$ with the lowest density crystalline material known ($0.17 \text{ g}/\text{cm}^3$).^{8–12} We are interested in COFs because they contain light elements (B, C, O, H, and Si). Such materials could be useful in automotive applications (storing CH_4 rather than gasoline¹³) and in CH_4 capture to prevent this greenhouse gas from getting into the atmosphere, of critical importance because methane is 21 times more effective in trapping heat in the atmosphere than CO_2 .¹⁴

We are also interested in the *delivery* amount of gas rather than the *excess* uptake because delivery is more important for industrial application. We define the delivery amount as the difference in the total amount adsorbed at certain pressure compared to the base pressure of the system, for example, atmospheric pressure.⁶ Much effort has been focused on reaching the DOE target of storing methane at 35 bar, because this is the pressure in natural gas pipelines. However, current commercial tanks can now hold pressures up to 250 bar, and hence we are interested in which frameworks are useful in this pressure range. Here we use virtual screening of candidate materials to discover new designs for COFs that can produce better CH_4 delivery methane uptake than current materials.

Our previous results showed that small pore diameter plus a high content of accessible aromatic rings give a heat of adsorption (Q_{st}) suitable for binding CH_4 at 298 K.⁶ On the other hand, too low a pore diameter leads to quick saturation at low pressures, as

was found for COF-1. We also found⁶ that methane–methane interactions are important in achieving good sorption performance with increasing pressure. On the basis of these lessons, we designed 15 new COFs containing alkyl substituents that we expected to take advantage of these interactions.

We based the new designs on building blocks with a 3,4-connectivity, shown previously to yield carbon–nitride (ctn) and boracite (bor) topologies.^{9,15,16} Figure 1 shows the building block used for this study as well as the chemistry of the condensation reactions. Scheme 1 summarizes the topologies and the kind of substituents used for the frameworks.

This paper is organized as follows. Section 2 describes the details about the methodology used for each simulation. It also includes the criteria used for the topological design of the new COFs. Section 3 presents the results about the volumetric delivery performances as well as Q_{st} values of our compounds versus representative COFs and MOFs without open metal sites (COF-102, COF-103, COF-105, COF-108, COF-202, MOF-177, and MOF-200). We also discussed the comparison of our results with previous studies. Finally, section 4 summarizes our main findings.

2. METHODOLOGY

2.1. Force Field. Nonbonding terms. Previously we developed a force field for nonbonded interactions (vdW-FF) of COFs and CH_4 based on quantum mechanics (QM) calculations at the MP2-IR/QZVPP level expected to be accurate for London dispersion forces (van der Waals attraction). We validated this

Received: October 3, 2011

Published: October 12, 2011

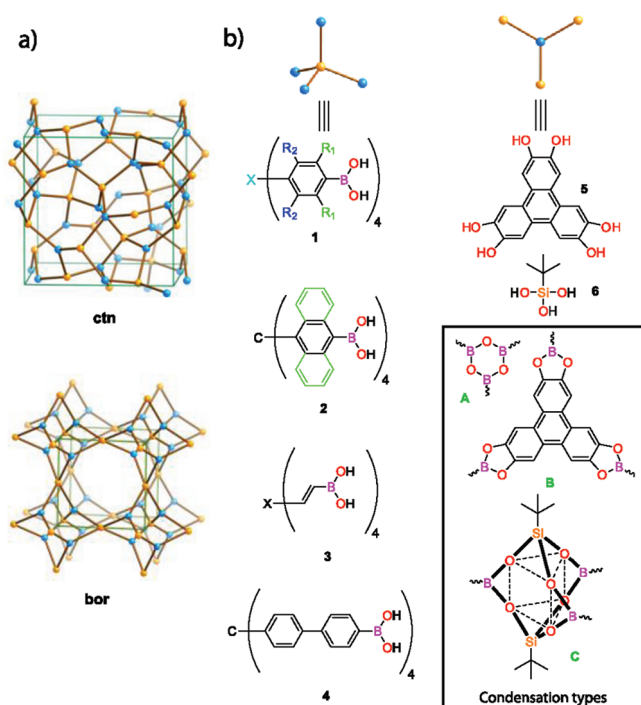


Figure 1. Building blocks used in this study for designing new COFs. The inset shows the types of condensation.

FF with the CH_4 equation of state at various temperatures (260–400 K) and pressures (1, 10, and 100 bar) and with experimental loading curves.⁶ This vdW-FF was used to calculate the loading curves.

Covalent Terms. For this work we are interested in studying the stability of the frameworks using molecular dynamics (MD). Thus we have combined our vdW-FF with the covalent terms from the DREIDING force field¹⁷ for use in the MD studies.

2.2. Electrostatic Interactions. We described the electrostatic interactions using the Mulliken charges from QM for the CH_4 molecule (C, -0.43820 ; H, $+0.10955$) and the QEq (charges equilibration) charges for the framework.¹⁸

2.3. Grand Canonical Monte Carlo. We used grand canonical Monte Carlo (GCMC) simulations to calculate the loading curves for these frameworks. Here we use our vdW-FF with QEq charges for the framework and QM charges for the CH_4 . At each pressure we considered 3 000 000 GCMC steps and tested that convergence was attained in each simulation. Every GCMC step allows four possible events: translation, rotation, creation, and annihilation each at equal probability.^{19,20} We used the GCMC code as implemented in Cerius2.

2.4. Molecular Dynamics. To test the stability of the compounds, we performed molecular dynamics (MD) simulations using the LAMMPS simulation engine with a 1 fs time step.²¹ We used the combined force field (vdW-FF plus Dreiding) to treat the interactions. The long-range electrostatics were treated using the particle–particle particle-mesh Ewald²² technique, with a real space cutoff of 10 Å and an accuracy tolerance of 10^{-5} . For each MD simulation we started with the equilibrium geometry from 500 steps of conjugated gradient (CG) minimization (cell coordinates and atom positions) followed by 10 ps of NVT dynamics to heat the system from 10 to 298 K. Finally, we ran NPT dynamics at 1 atm and 298 K for 7.5 ns from which we collect all relevant data. The temperature damping constant was

Scheme 1. Reactions Involving the New COFs^a

Reactants	Type	R_1	R_2	Name	topology
1	A	X=C	—H	COF-102	ctn
1	A	X=C	— CH_2CH_3	COF-102-Et-H	ctn
1	A	X=C	— $\text{CH}(\text{CH}_3)_2$	COF-102-iPr-H	ctn
1	A	X=C	— $(\text{CH}_2)_2\text{CH}_3$	COF-102-Pr-H	ctn
1	A	X=C	— $\text{C}(\text{CH}_3)_3$	COF-102-tBu-H	ctn
1	A	X=C	— CH_3	COF-102-Me-Me	ctn
1	A	X=Si	— CH_3	COF-103-Me-Me	ctn
2	A	X=C	N/A	COF-102-Ant	ctn
3	A	X=C	N/A	COF-102-Eth-cis	ctn
3	A	X=Si	N/A	COF-103-Eth-cis	ctn
5+1	B	X=Si	— CH_3	COF-105-Me-Me	ctn
5+1	B	X=C	—H	COF-108	bor
5+1	B	X=C	— $(\text{CH}_2)_2\text{CH}_3$	COF-108-nHex-H	bor
5+1	B	X=C	— CH_3	COF-108-Me-Me	bor
5+3	B	X=C	N/A	COF-105-Eth-cis	ctn
6+1	C	X=C	—H	COF-202	ctn
6+4	C	X=C	—H	COF-212	ctn

^aThe first column shows the building blocks used and the second column shows the type of condensation undergone. Note that between COF-102 and COF-103 analogs the only difference is the central atoms of the tetrahedral, C and Si, respectively.

0.1 ps, and the pressure damping constant was 2.0 ps. The equations of motion used are those of Shinoda et al.,²³ which combine the hydrostatic equations of Martyna et al.²⁴ with the strain energy proposed by Parrinello and Rahman.²⁵ The time integration schemes closely follow the time-reversible measure-preserving Verlet integrators derived by Tuckerman et al.²⁶

2.5. Topological Consideration in the Design of COFs. For the design of the 3,4 frameworks we used only the ctn ($I\bar{4}3d$ space group) and bor ($P\bar{4}3m$ space group) topologies because they have been shown to be the most stable.^{9,15,16} To build each structure, we used the corresponding space group and add the irreducible representation of the ligand into it. None of the ligands produces lower symmetry frameworks.

We minimize these frameworks with CG for 500 steps, which always led to convergence. During the design of COF-102-Eth-trans, COF-103-Eth-trans, and COF-105-Eth-trans, we found that the cis version is incompatible with these constraints and that the framework is unstable after minimization, leaving the trans isomer as the only choice. The optimized structures coordinates are reported in the Supporting Information.

3. RESULTS AND DISCUSSION

3.1. Delivery Volumetric Uptake in Designed COFs. The DOE goal for methane storage is $180 v(STP)/v$ at 35 bar. Here, $v(STP)/v$ denotes the volume of methane per volume of system, where STP is the standard temperature and pressure of 298 K and 1.01 bar.²⁷ Only two materials have been reported to satisfy the methane uptake DOE requirements at 35 bar: Ni-MOF-74 and PCN-14. In the experimental reports, 1 atm and 273 K were used as the standard units. Thus, Ni-MOF-74²⁸ reached 190 excess $v(273 \text{ K}, 1 \text{ atm})/v$ and PCN-14²⁹ reached 220 excess $v(273 \text{ K}, 1 \text{ atm})/v$, the latter measured at 290 K. To make a fair comparison in the following discussions, we multiply these experimental quantities by 1.09 (or 298/273) to get our defined STP . Therefore, after conversion, we obtain 207 $v(STP)/v$ for Ni-MOF-74 and 240 $v(STP)/v$ for PCN-14.

The representative MOF-177,³⁰ which is now in industrial production for automotive applications,³¹ achieves only 91

Table 1. Isotheric Heat of Adsorption (Q_{st}), Surface Area (S_A), Pore Volume (V_p), and Uptake of the Framework Series at 298 K (Where Tot = Total, Exc = Excess, and Eel = Delivery)^a

material	Q_{st} (kJ/mol)	S_A (m ² g ⁻¹)	V_p (cm ³ g ⁻¹)	TotCH ₄ [v(STP)/v]	ExcCH ₄ [v(STP)/v]	DelCH ₄ [v(STP)/v]	DelCH ₄ [v(STP)/v]
				at 35 bar	at 35 bar	at 35 bar	at 300 bar
PCN-14 ²⁹	30.0	1753	0.87	251 ^b (230 ^c)	240 ^b (220 ^c)		
Ni-MOF-74 ²⁸	20.2	1033	0.54	218 ^b (200 ^c)	207 ^b (190 ^c)		
COF-1	25.1	1230	0.38	196	196	145	150
COF-102	10.5	4940	1.81	143	120	137	340
COF-102-Ant	18.4	2720	0.75	215	200	180	258
COF-102-Eth-trans	13.1	4640	1.20	184	166	172	306
COF-103-Eth-trans	13.3	4920	1.36	206	187	192	328
COF-105-Eth-trans	9.3	6350	3.62	114	86	110	350
MOF-177	9.6	4800	1.93	116	91	112	336
MOF-200	7.9	5730	4.04	84	54	81	321
Pure CH ₄	3.0			35		34	263

^a Q_{st} values are reported as an average from 1 to 300 bar. S_A and V_p were estimated from rolling an Ar molecule with diameter of 3.42 Å⁶ over the framework's surface. The GCMC predicts an uncertainty of 2% in our reported uptakes but for clarity it is not shown. For PCN-14 and Ni-MOF-74 we use the experimental Q_{st} at low pressure (nearly zero coverage).^{28,29} The S_A and V_p for PCN-14 and Ni-MOF-74 were also obtained from literature.^b We have converted the experimental uptake (273 K, 1 atm) to our STP units (298 K, 1.01 bar) by multiplying by the factor 1.09 to get a better comparison.^c Experimental value (273 K, 1 atm).^{28,29}

excess v(STP)/v at 35 bar. The excess and total uptakes are summarized in Table 1, where we used standard definitions for these quantities.^{4,32} We use only experimental uptakes for PCN-14 and Ni-MOF-74 because our vdW-FF does not deal yet with open metal sites.

The results for the delivery amount of methane for our four best new designs for up to 35 bar are shown in Figure 2, whereas the performance for the remaining 11 systems are in the Supporting Information. At 35 bar (in v(STP)/v delivery units) the best performers are

- COF-103-Eth-trans (192 ± 4), exceeding the DOE target,
- COF-102-Ant (180 ± 3),
- COF-102-Eth-trans (172 ± 3), and
- COF-105-Eth-trans (110 ± 2).

Thus COF-103-Eth-trans stores 5.6 times as much as bulk CH₄ at the same pressure (bulk CH₄ reaches 34 ± 1). All our designed COFs have superior performance to previously reported COFs and MOFs, such as COF-102 (137 ± 3), MOF-177 (112 ± 2), and MOF-200 (81 ± 2).

The new materials were designed for best performance at 35 bar. At higher pressures, the trend in performance (at 300 bar and in v(STP)/v delivery units) changes:

- COF-105-Eth-trans (350 ± 7),
- COF-103-Eht-trans (328 ± 7),
- COF-102-Eht-trans (306 ± 6), and
- COF-103-Ant (258 ± 5)

Therefore, at 300 bar, COF-105-Eth-trans stores 1.3 times as much as an empty container (bulk CH₄ takes 263 ± 3). Other good performers over the range of 1–300 bar are shown in the Supporting Information. For example, at 300 bar, COF-103 reaches 352 ± 7 delivery v(STP)/v, followed by COF-105 (327 ± 7), COF-108 (318 ± 6), COF-212 (310 ± 6), COF-105-Met-Met (308 ± 6), and COF-108-Met-Met (302 ± 6). We see that some of these new designs perform better than the archetypal frameworks: COF-102 (340 ± 7), MOF-177 (336 ± 7), and MOF-200 (321 ± 6). Figure 2 shows that COF-102-Ant performs comparable to bulk CH₄ container at 300 bar whereas under 35 bar it approaches the DOE target.

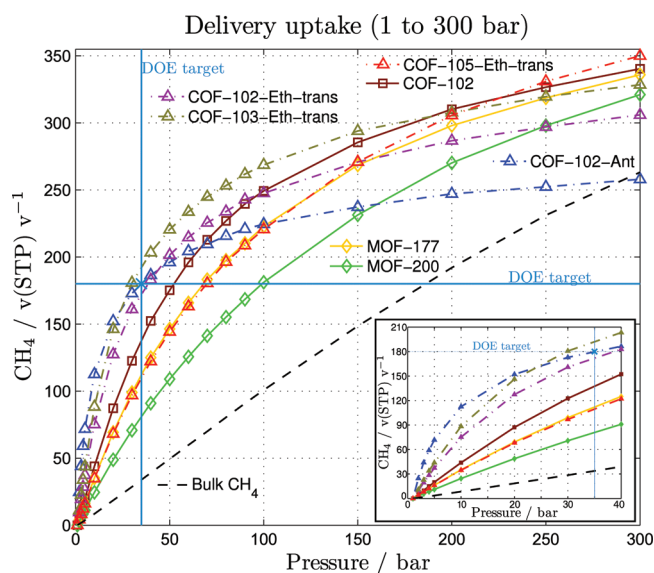


Figure 2. CH₄ uptake for the best COF performers. The delivery amount using a base pressure of 1 bar is reported. The best performers at 35 bar are shown along with some that perform best at 300 bar. Solid lines indicate published compounds.

Our results show that attaching alkyl substituents such as –CH₃, –CH₂CH₃, –CH₂CH₂CH₃, –CH₂(CH₃)₂, –C(CH₃)₃, or –(CH₂)₅CH₃ to the benzene rings does not increase the binding over having the simple H substituent. Among alkyl-substituted benzenes, the type of isomer matters because the one with higher surface area performs better, in particular when propyl (2590 m²/g) and isopropyl (1420 m²/g) are compared. The propyl substituent has a higher uptake when compared to isopropyl because more atoms are available to interact with a sorbent molecule and gives higher surface area even though they have the same components.

3.2. Isotheric Heat of Adsorption. Our calculated Q_{st} values are shown in Figure 3. These trends can be understood from a

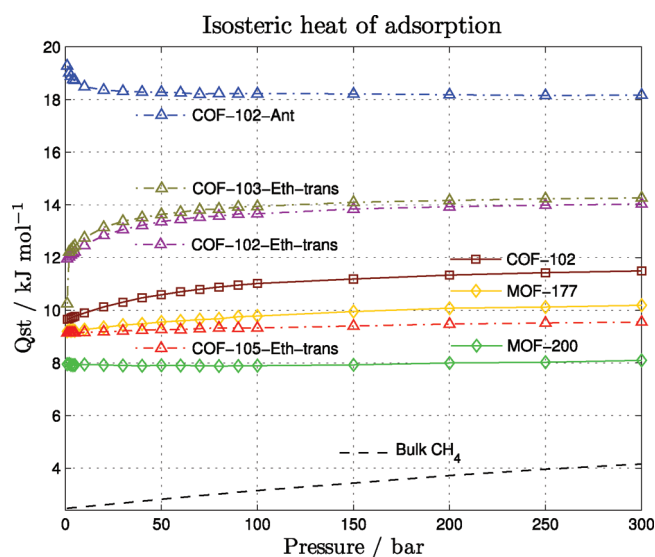


Figure 3. Heat of adsorption calculated for the compounds in Figure 2. The results for the remaining compounds are in the Supporting Information.

comparison of COF-1, COF-102-Ant, and COF-103-Eth-trans (Table 1). COF-1 has the highest Q_{st} among COFs, but it is saturated by 40 bar, giving the poorest delivery uptake. COF-102-Ant outperforms COF-1 despite a smaller Q_{st} value due to the higher S_A and V_p . Finally, COF-103-Eth-trans is the best performer due to its balance of mild Q_{st} , high S_A and high V_p .

High Q_{st} (>20 kJ/mol) at low pressures and low S_A and V_p lead to low delivery amount. The same analysis was done for PCN-14 and Ni-MOF-74 where experiments found high Q_{st} (30.0 and 20.2 kJ/mol, respectively, at nearly 0 bar) but poor S_A (1753 and 1033 m²/g, respectively) and V_p (0.87 and 0.54 cm³/g, respectively). Thus we expect that PCN-14 and Ni-MOF-74 will saturate by 100 bar, consistent with their experimental sorption isotherm curves trend. We did not simulate PCN-14 and Ni-MOF-74 in this study because we have not yet developed a FF to deal with the open metal sites, which are an important feature in these compounds. The trends in performance at higher pressure are also shown for archetypal MOF-177 and MOF-200, which have lower Q_{st} of 9.7 ± 0.5 and 8.0 ± 0.2 , respectively. However, the higher S_A (4800 and 5730 m²/g, respectively) and V_p (1.93 and 4.04 cm³/g, respectively) give them an advantage at pressure beyond 100 bar.

In this work we are focused on getting the best performance in delivery units and this requires a low interaction methane-COF in the low-pressure range. In other words, we want to get a low Q_{st} at low pressure. We have succeeded in obtaining this behavior for COF-102-Eth-trans and COF-103-Eth-trans by using the tiny vinyl link, as demonstrated by the shape of their Q_{st} curves, which are similar to that of COF-102 but more marked for the entire pressure range. Eventually, methane–methane interactions compensate to show moderate Q_{st} . This is opposite to the Q_{st} profile of COF-102-Ant where the link being used gives a high interaction at low loading (Figure 3). Therefore, our new designs using vinyl linkers present a new way to maximize delivery uptake, which is different from the approach of using fused phenyl rings.

3.3. Stability of COFs. Recently, it was suggested³³ that COF-108 and even COF-102 might collapse due to instability of the

Table 2. MD statistics for the frameworks obtained at 298 K.^a

material	MD _{lattice} (Å)	MD _{std dev} (%)	Exp _{lattice} (Å)
COF-102	27.444	0.0268 (0.098)	27.177
COF-103	27.860	0.0280 (0.101)	28.248
COF-108	28.917	0.0402 (0.139)	28.401
COF-102-Ant	27.759	0.0389 (0.140)	
COF-102-Eth-trans	19.820	0.0274 (0.138)	
COF-103-Eth-trans	20.371	0.0290 (0.142)	
COF-105-Eth-trans	37.043	0.0483 (0.130)	
MOF-5	24.286	0.0533 (0.219)	25.790 (0.46%) ^b

^a The standard deviation was calculated after 10 ps. All these frameworks have a cubic lattice. ^b The experimental lattice value for MOF-5 is taken as the median of most representative experimental conditions reported (the average for these experiments is 25.833 Å). For comparison we show in parentheses the percentage from upper and bottom bounds.^{34–36}

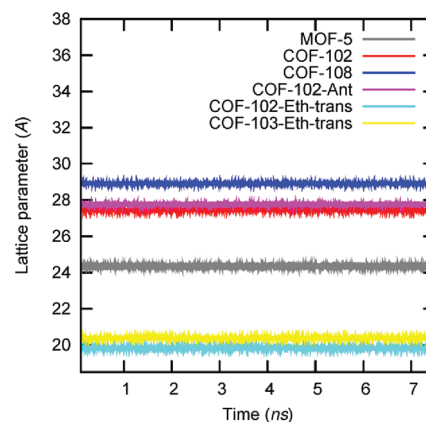


Figure 4. Lattice parameter variations obtained from MD for several COFs. The lattice parameters are in Angstroms (Å) and time in nanoseconds (ns). COF-103 and COF-105-Eth-trans are not shown; the statistics are summarized in Table 2.

frameworks; however, the same study suggested that for COF1 the “AA” conformation is more stable than the experimentally observed “AB” conformer.³³ Therefore, we decided to study the stability of our newly designed COFs with MD simulations. Our results show that cell parameters of our new COFs change only slightly (0.130–0.142%) throughout the entire dynamics while the cell angles stayed at 90° (orthorhombic) as shown in Table 2 and Figure 4.

For comparison, we also performed MD on the characteristic MOF-5 because it is very well documented experimentally that the lattice parameters change from 25.670 to 25.910 Å over a temperature range of 3.5–300 K but remain stable under these conditions.^{34–36} We find that MOF-5 has a change of 0.219% in the lattice parameters, larger than our new COFs (Table 2). This indicates that our new COFs and the experimental COFs are stable without guest molecules at 298 K and 1 atm.

3.4. Comparisons to Previous Computational Studies. A previous computational report about sorption of CH₄ on MOFs showed that increasing the number of fused benzene rings increases the Q_{st} value.³⁷ However, they reported that their empirical vdW attraction terms led to errors of 5.7–9.9% greater than experiments. This study did not report the stability of their designed compound IRMOF-993, and experimentalists

attempted to synthesize the proposed IRMOF-993 but could only create the analog PCN-13. The synthesized framework has the same components but a different topology with a smaller pore size (almost half of the originally proposed MOF-993).³⁸ MOF-993 was reported to be topologically stable on the basis of studies of Snurr et al.,³⁷ however, it was found by experimentalists not to be thermodynamically accessible. Even so, these studies showed that enhancement of CH₄ storage at pressures below 35 bar on MOFs can be attained by increasing the Q_{st} value by putting fused rings into the framework, assuming the structure is stable. Our study shows that this is also the case for CH₄ in COFs; however, we found that this is a poor strategy if we want to obtain a good delivery uptake at higher pressures and it does not help beyond 250 bar.

To avoid such problems, we performed MD calculations on our proposed topological stable frameworks to show that they are also dynamically stable. Our current study shows that enhancement of the CH₄ delivery amount can be attained reducing the interaction at low-pressure of methane-COF while also demonstrating stability of the proposed frameworks. We found that this behavior is opposite to that of putting fused benzene rings when looking at the interaction profile over the entire pressure range.

4. CONCLUDING REMARKS

In summary, we have also shown two ways to produce improved absorbents for higher delivery methane up to 35 bar:

- by using skinny ligands to minimize the methane-COF interaction in the low-pressure range (COF-102-Ethtrans and COF-103-Eth-trans) and
- by increasing the heat of adsorption (COF-102-Ant).

We also found that the performance at 300 bar can be improved by frameworks with larger pore volumes and surface areas. Our results show that attaching systematically alkyl substituents to the benzene rings does not increase the binding over having a simple -H substituent. These conclusions should apply also to metal-organic frameworks and zeolite imidazolate frameworks.

■ ASSOCIATED CONTENT

S Supporting Information. Properties (surface area, pore volume, density) for all the analyzed frameworks, volumetric uptake for using 1 and 5 bar as the basis, and isosteric heat of adsorption are included. We also include the expanded version of frameworks presented here. 3D representations and crystal data. This material is free of charge vide the Internet at <http://pubs.acs.org>. This material is available free of charge via the Internet at <http://pubs.acs.org>.

■ AUTHOR INFORMATION

Corresponding Author

*E-mail: wag@wag.caltech.edu. Phone: 626-395-2731. Fax: 626-585-0918.

■ ACKNOWLEDGMENT

We thank Prof. Omar Yaghi and Dr. Hiroyasu Furukawa for many helpful suggestions and comments. J.L.M.-C. acknowledges the Roberto Rocca Fellowship for partial financial support. This project was funded by a grant (DE-FG01-04ER0420) for

the U.S. Department of Energy. The computer facilities of the Materials and Process Simulation Center were supported by ONR-DURIP and ARO-DURIP.

■ REFERENCES

- (1) Furukawa, H.; Yaghi, O. M. *J. Am. Chem. Soc.* **2009**, *131*, 8875–8883.
- (2) Han, S. S.; Furukawa, H.; Yaghi, O. M.; Goddard, W. A. *J. Am. Chem. Soc.* **2008**, *130*, 11580.
- (3) Kaye, S. S.; Dailly, A.; Yaghi, O. M.; Long, J. R. *J. Am. Chem. Soc.* **2007**, *129*, 14176–14177.
- (4) Furukawa, H.; Miller, M. A.; Yaghi, O. M. *J. Mater. Chem.* **2007**, *17*, 3197–3204.
- (5) Millward, A. R.; Yaghi, O. M. *J. Am. Chem. Soc.* **2005**, *127*, 17998–17999.
- (6) Mendoza-Cortes, J. L.; Han, S. S.; Furukawa, H.; Yaghi, O. M.; Goddard, W. A. *J. Phys. Chem. A* **2010**, *114*, 10824–10833.
- (7) Eddaoudi, M.; Kim, J.; Rosi, N.; Vodak, D.; Wachter, J.; O’Keeffe, M.; Yaghi, O. M. *Science* **2002**, *295*, 469–472.
- (8) Cote, A. P.; Benin, A. I.; Ockwig, N. W.; O’Keeffe, M.; Matzger, A. J.; Yaghi, O. M. *Science* **2005**, *310*, 1166–1170.
- (9) El-Kaderi, H. M.; Hunt, J. R.; Mendoza-Cortes, J. L.; Cote, A. P.; Taylor, R. E.; O’Keeffe, M.; Yaghi, O. M. *Science* **2007**, *316*, 268–272.
- (10) Cote, A. P.; El-Kaderi, H. M.; Furukawa, H.; Hunt, J. R.; Yaghi, O. M. *J. Am. Chem. Soc.* **2007**, *129*, 12914–12915.
- (11) Hunt, J. R.; Doonan, C. J.; LeVangie, J. D.; Cote, A. P.; Yaghi, O. M. *J. Am. Chem. Soc.* **2008**, *130*, 11872–11873.
- (12) Furukawa, H.; Ko, N.; Go, Y. B.; Aratani, N.; Choi, S. B.; Choi, E.; Yazaydin, A. O.; Snurr, R. Q.; O’Keeffe, M.; Kim, J.; Yaghi, O. M. *Science* **2010**, *329*, 424–428.
- (13) Celzard, A.; Fierro, V. *Energy Fuels* **2005**, *19*, 573–583.
- (14) Lelieveld, J.; Crutzen, P. J.; Dentener, F. J. *Tellus Ser. B-Chem. Phys. Meteorol.* **1998**, *50*, 128–150.
- (15) Delgado-Friedrichs, O.; O’Keeffe, M.; Yaghi, O. M. *Acta Crystallogr., Sect. A* **2006**, *62*, 350–355.
- (16) Schmid, R.; Tafipolsky, M. *J. Am. Chem. Soc.* **2008**, *130*, 12600–12601.
- (17) Mayo, S. L.; Olafson, B. D.; Goddard, W. A. *J. Phys. Chem.* **1990**, *94*, 8897–8909.
- (18) Rappe, A. K.; Goddard, W. A. *J. Phys. Chem.* **1991**, *95*, 3358–3363.
- (19) Adams, D. J. *Mol. Phys.* **1974**, *28*, 1241–1252.
- (20) Soto, J. L.; Myers, A. L. *Mol. Phys.* **1981**, *42*, 971–983.
- (21) Plimpton, S. J. *Comput. Phys.* **1995**, *117*, 1–19.
- (22) Plimpton, S. J.; Pollock, R.; Stevens, M. In *Proceedings of the Eighth SIAM Conference on Parallel Processing for Scientific Computing*; Minneapolis, MN, 1997.
- (23) Shinoda, W.; Shiga, M.; Mikami, M. *Phys. Rev. B* **2004**, *69*, 1341031–1341038.
- (24) Martyna, G. J.; Tobias, D. J.; Klein, M. L. *J. Chem. Phys.* **1994**, *101*, 4177–4189.
- (25) Parrinello, M.; Rahman, A. *J. Appl. Phys.* **1981**, *52*, 7182–7190.
- (26) Tuckerman, M. E.; Alejandre, J.; Lopez-Rendon, R.; Jochim, A. L.; Martyna, G. J. *J. Phys. a—Math. Gen.* **2006**, *39*, 5629–5651.
- (27) Burchell, T. *SAE Tech. Pap.* **2000**, *01*, 2205.
- (28) Wu, H.; Zhou, W.; Yildirim, T. *J. Am. Chem. Soc.* **2009**, *131*, 4995–5000.
- (29) Ma, S. Q.; Sun, D. F.; Simmons, J. M.; Collier, C. D.; Yuan, D. Q.; Zhou, H. C. *J. Am. Chem. Soc.* **2008**, *130*, 1012–1016.
- (30) Chae, H. K.; Siberio-Perez, D. Y.; Kim, J.; Go, Y.; Eddaoudi, M.; Matzger, A. J.; O’Keeffe, M.; Yaghi, O. M. *Nature* **2004**, *427*, 523–527.
- (31) Czaja, A. U.; Trukhan, N.; Muller, U. *Chem. Soc. Rev.* **2009**, *38*, 1284–1293.
- (32) Zhou, W.; Wu, H.; Hartman, M. R.; Yildirim, T. *J. Phys. Chem. C* **2007**, *111*, 16131–16137.
- (33) Zhou, W.; Wu, H.; Yildirim, T. *Chem. Phys. Lett.* **2010**, *499*, 103–107.

- (34) Li, H.; Eddaoudi, M.; O’Keeffe, M.; Yaghi, O. M. *Nature* **1999**, *402*, 276–279.
- (35) Rowsell, J. L. C.; Spencer, E. C.; Eckert, J.; Howard, J. A. K.; Yaghi, O. M. *Science* **2005**, *309*, 1350–1354.
- (36) Yildirim, T.; Hartman, M. R. *Phys. Rev. Lett.* **2005**, *95*.
- (37) Duren, T.; Sarkisov, L.; Yaghi, O. M.; Snurr, R. Q. *Langmuir* **2004**, *20*, 2683–2689.
- (38) Ma, S. Q.; Wang, X. S.; Collier, C. D.; Manis, E. S.; Zhou, H. C. *Inorg. Chem.* **2007**, *46*, 8499–8501.